Journal of Beijing Institute of Technology, 2021, Vol. 30, Suppl.1

Electro-Hydraulic Proportional Position Control Using Auto Disturbance Rejection Based on RBF Neural Network

Xiwei Peng[1], Haiyang Yu[2], Xiangjie Zhu[3] and Yiran Li✉

(1. School of Automation, Beijing Institute of Technology, Beijing 100081, China; 2. Cambricon Technologies Corporation Limited, Beijing 100191, China; 3. System Engineering Research Institute of China State Shipbuilding Corporation, Beijing 100094, China)

Abstract: Large friction force and large dead zone are two typical nonlinear characteristics of electro-hydraulic proportional valve controlled hydraulic cylinder position control system. Aiming at those characteristics, a dead zone dynamic compensation algorithm is researched in order to reduce the lag time and control error. At the same time, a control strategy of radial basis function (RBF) neural network combined with auto disturbance rejection control (ADRC) is researched according to the impact of different conditions. The experimental result shows that the proposed algorithm improves performance of the electro-hydraulic proportional valve controlled hydraulic cylinder position control system. In positioning control experiment, the overshoot is 0 and the stability error is 0. In tracking control experiment, the lag time is reduced from the original 1.5 s to 0.2 s with no flat top phenomenon and the maximum error was reduced from 20 mm to 3 mm.

Key words: proportional valve controlled hydraulic cylinder; auto disturbance rejection control (ADRC); radial basis function (RBF) neural network; dead zone

CLC number: TP273 **Document code:** A **Article ID:** 1004-0579(2021)S1-0121-08

Electro-hydraulic proportional control technology is widely used in metallurgy, construction machinery, automatic production and other fields because of its strong anti-pollution ability, high reliability, low cost and simple maintenance. However, the negative impacts of dead zone, friction and other nonlinear characteristics, the control accuracy and response speed are significantly affected, so that the traditional PID control is difficult to meet high performance requirements. With the rapid development of computer technology, intelligent control theories such as fuzzy control, sliding-mode control, iterative control, active disturbance rejection control(ADRC) and neural network control have been applied to electro-hydraulic proportional control system.

ADRC is model-free, predictive and robust, which has been applied in many fields. Flight propulsion control is solved by ADRC[1], and the automatic login of aircraft by ADRC is studied[2]. Ref.[3] overcomes strong nonlinearity and external disturbance through ADRC, and obtains better current conversion results. ADRC technology is applied on the study of maximum wind energy control[4]. Also, ADRC is successfully applied to permanent magnet synchronous motor servo system[5] and track control of maglev train[6]. ADRC is applied in the electro-hydraulic servo control system[7], in which total disturbance estimation is used to effectively compensate the system control, and fast response, no overshoot, and high steady-state accuracy are obtained, where internal and external disturbances have strong suppres-

Received 2020-07-29
✉ Author for correspondence
E-mail: labiding@163.com
DOI: 10.15918/j.jbit1004-0579.20098

sion ability. ADRC is adopted to speed up the response of electro-hydraulic servo system, and the effectiveness of the control strategy is proved by simulation of local impact disturbance[8].

ADRC is model-free and has a quick and accurate control performance for nonlinear complex system. However, the algorithm is difficult to adjust because of too many parameters. In order to solve the deficiency of the accuracy of artificial parameter adjustment, some scholars also adopt the combination of neural network and ADRC control to optimize the parameters of the control algorithm. Neural network is applied to tune three parameters automatically and car transmission, which could well adapt to road conditions and improve the smoothness of gear shift[9]. Neural network is also applied to tune PID parameters and optimize the temperature control systems[10].

In this paper a radial basis function (RBF) neural network based ADRC (RBF-ADRC) combined with dead zone dynamic compensation control strategy is proposed to solve electro-hydraulic proportional position control with large error in dead zone. The predictive of ADRC is used for system state observation, as well as RBF neural network is used for ADRC parameter optimization, so that to realize a fast tracking and precise control system[11].

1 Working Principle of Hydraulic Cylinder System

The electro-hydraulic proportional valve-controlled hydraulic cylinder system is mainly composed of oil source, hydraulic cylinder, position detection element, controller, upper computer, proportional amplifier, electro-hydraulic proportional valve, etc., as shown in Fig. 1.

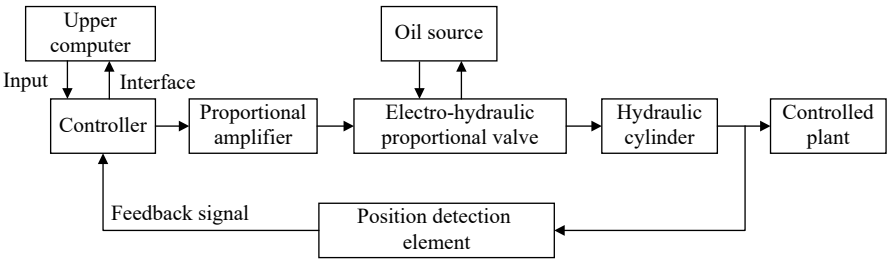

Fig. 1 Block diagram of system

To described each element in the system, and combine them together as a system. The system's transfer function block diagram is obtained, as shown in Fig. 2.

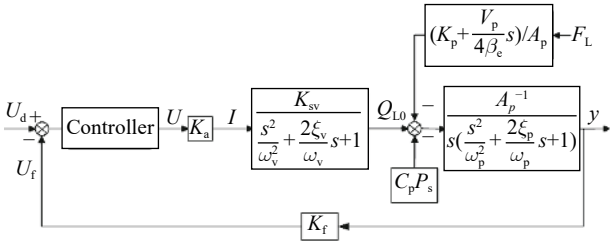

Fig. 2 Transfer function diagram of system

According to the transfer function block diagram in Fig. 2, the open-loop transfer function of the system is derived as

$$G(s)=\frac{Y(s)}{U(s)}=\frac{K_{sv}K_aK_f/A_p}{s\left(\frac{s^2}{\omega_v^2}+\frac{2\xi_v}{\omega_v}s+1\right)\left(\frac{s^2}{\omega_p^2}+\frac{2\xi_p s}{\omega_p}+1\right)}=\frac{K_{sys}}{s\left(\frac{s^2}{\omega_v^2}+\frac{2\xi_v}{\omega_v}s+1\right)\left(\frac{s^2}{\omega_p^2}+\frac{2\xi_p s}{\omega_p}+1\right)} \tag{1}$$

where $K_{sys}=K_{sy}K_aK_f/A_p$ is the open-loop gain of the system, affecting system's stability and response speed.

2 System Control Strategy

To get a prefect control performance, a dead zone dynamic compensation and RBF neural network based ADRC algorithm is designed to realize perfect control of electro-hydraulic propor-

tional valve-controlled hydraulic cylinder position servo system.

2.1 Dynamic dead zone compensation strategy

The flow characteristic curve of proportional valve used in this paper is shown in Fig. 3. When the input signal is more than 20%, the valve eloquence will have the flow through, using the simple dead zone fixed value compensation and linear compensation, the control effect is not ideal, so a dynamic compensation strategy is proposed.

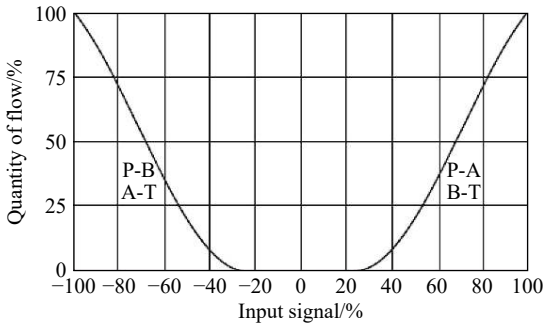

Fig. 3 Flow characteristic curve of proportional valve

The dynamic compensation strategy is based on the real-time position of the hydraulic cylinder (error size).

Assume the output control signal is U_c, the dead zone compensation is U_d, so the total output control signal of the controller is $U = U_c + U_d$. Let the position error of the hydraulic cylinder be e and the allowable error is e_{min}. According to Fig. 3, the dead zone value is obtained according to 20% maximum current value of the valve port U_l, a and b are the amplification factors.

In view of the asymmetric characteristics of the hydraulic cylinder, different amplification factors a and b (range between 1 and 2) are adopted to ensure the real-time tracking performance and stability of control system when the hydraulic rod is transferred between extended state to retractable state.

Dynamic dead zone compensation strategy is designed as follows

① When $|e| \le e_{min}$, the control accuracy has been achieved, $U_d = 0$.

② When $|e| > e_{min}$, if $U_c > 0$, then $U_d = U_l$; if $U_c < 0$, then $U_d = aU_l$.

③ When $e < -e_{min}$, if $U_c < 0$, then $U_d = -U_l$, if $U_c > 0$, then $U_d = -bU_l$.

2.2 RBF neural network based ADRC algorithm

The RBF neural network based ADRC control system is shown in Fig. 4. The RBF neural network is used to quickly approximate the nonlinear function and self-learning ability. After issuing the command signal, the motion change information of the device can be tracked without lag, and the information can be quickly provided to the ADRC controller, so as to realize the fast parameter adjustment of the controller.

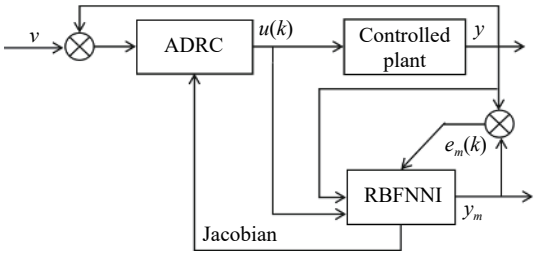

Fig. 4 RBF neural network based ADRC system

2.2.1 RBF neural network identifier (RBFNNI)

The proposed RBF neural network structure 3-6-1 is shown in Fig. 5.

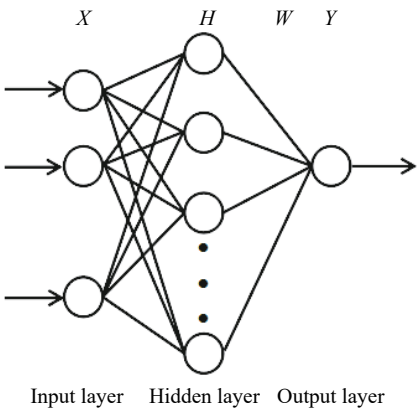

Fig. 5 RBF neural network structure diagram

Let $\boldsymbol{x} = [u(k), y(k), y(k-1)]^T$ is the input value of three input nodes, $\boldsymbol{h} = [h_1, h_2, h_3, h_4, h_5, h_6]$ is the radial basis function of six hidden layer nodes realized by Gaussian function.

$$\boldsymbol{h}_j = \exp\left(-\frac{\|\boldsymbol{X} - \boldsymbol{C}_j\|^2}{2b_j^2}\right), \quad j = 1, 2, \cdots, 6 \quad (2)$$

where $\boldsymbol{C}_j$ is the center vector of j node of the hidden layer network, $\boldsymbol{B}=[b_1,b_2,b_3,b_4,b_5,b_6]$ is the width vector of the network, $b_j>0$ is the basis width parameter of the j node, $\boldsymbol{W}=[w_1,w_2,w_3,w_4,w_5,w_6]$ is the linear weight ratio from the hidden layer to the output layer. The output of RBF neural network identifier is formulated as

$$y_{\mathrm{m}}(k)=w_1h_1+w_2h_2+w_3h_3+w_4h_4+w_5h_5+w_6h_6 \quad (3)$$

The gradient descent method is adopted in the classifier, and the criterion function is

$$J(w)=\frac{1}{2}(y(k)-y_{\mathrm{m}}(k))^2 \quad (4)$$

where $J(w)$ represents criterion function value; $y(k)$ is expected output, $y_{\mathrm{m}}(k)$ represents the actual output, w is the vector of ownership values. The basic principle of the algorithm is to modify the parameters $w(k)$ of the model gradually along the negative gradient direction of the function until $J(w)$ reaches the minimum.

The output of neural network could be regarded as a function of neural network weight vector $\boldsymbol{w}$, where the ultimate goal of network learning is to make the square value of $y(k)-y_{\mathrm{m}}(k)$ infinitely close to zero, that is, $J(w)$ infinitely close to zero, so as to modify the network weight vector.

According to this idea, the iterative algorithm for adjusting center parameters, base width and linear weight ratio of each node in the neural network is

$$\Delta c_{ji}=(y(k)-y_{\mathrm{m}}(k))w_j\frac{x_j-c_{ji}}{b_j^2} \quad (5)$$

$$c_{ji}(k)=c_{ji}(k-1)+\eta\Delta c_{ji}+\alpha(c_{ji}(k-1)-c_{ji}(k-2)) \quad (6)$$

$$\Delta b_j=(y(k)-y_{\mathrm{m}}(k))w_jh_j\frac{|X-C_j|^2}{b_j^3} \quad (7)$$

$$b_j(k)=b_j(k-1)+\eta\Delta c_j(k)+\alpha(b_j(k-1)-b_j(k-2)) \quad (8)$$

$$\Delta w_j=(y(k)-y_{\mathrm{m}}(k))h_j \quad (9)$$

$$w_j(k)=w_j(k-1)+\eta\Delta w_j(k)+\alpha(w_j(k-1)-w_j(k-2)) \quad (10)$$

where η is learning rate, α is momentum factor. The identification information of the network identifier would be transmitted to the ADRC to tune the controller parameters. The Jacobian matrix is shown as

$$\frac{\partial y(k)}{\partial u(k)}\approx\frac{\partial y_{\mathrm{m}}(k)}{\partial u(k)}=\sum_{j=1}^{6}w_jh_j\frac{c_{j1}-x_1}{b_j^2} \quad (11)$$

where $x_1=u(k)$.

2.2.2 Design of ADRC controller

ADRC is mainly composed of three parts: the track-differentiator, the extended state observer and the nonlinear state error feedback control law as shown in Fig. 6.

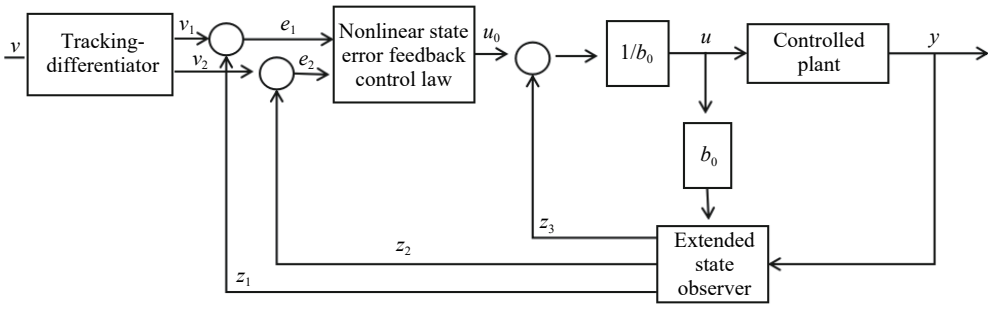

Fig. 6 ADRC basic structure

The nonlinear tracking-differentiator transition process is

$$\begin{cases}\mathrm{fh}=\mathrm{fhan}(x_1(k)-v(k),x_2(k),r,h_0)\\ x_1(k+1)=x_1(k)+hx_2(k)\\ x_2(k+1)=x_2(k)+h\mathrm{fh}\end{cases} \quad (12)$$

where v is the input signal, x_1 realizes the fast overshoot tracking to v, x_2 is the approximate differential signal of v, h is the sampling period of the object, fhan is the fastest synthesis function.

$$\begin{cases} d = rh_0^2 \\ a_0 = h_0 x_2 \\ y = x_1 + a_0 \\ a_1 = \sqrt{d(d+8|y|)} \\ a_2 = a_0 + \text{sign}(y)(a_1 - d)/2 \\ s_y = [\text{sign}(y+d) - \text{sign}(y-d)]/2 \\ a = (a_0 + y - a_2)s_y + a_2 \\ s_a = [\text{sign}(a+d) - \text{sign}(a-d)]/2 \\ \text{fhan} = -r[a/d - \text{sign}(a)]s_a - r\text{sign}(a) \end{cases} \quad (13)$$

where x_1,x_2 is the states of system; r,h_0 is the control parameters of the function. The expanded state observer is

$$\begin{cases} \varepsilon_1 = z_1(k) - y(k) \\ z_1(k+1) = z_1(k) + h[z_2(k) - \beta_{01}\varepsilon_1] \\ z_2(k+1) = z_2(k) + h[z_3(k) - \beta_{02}\text{fal}(\varepsilon_1, \alpha_1, \delta) + bu] \\ z_3(k+1) = z_3(k) - h\beta_{03}\text{fal}(\varepsilon_1, \alpha_2, \delta) \end{cases} \quad (14)$$

where β_{01}, β_{02}, β_{03} is the adjustment parameter, fal() is nonlinear function formulated as

$$\text{fal}(\varepsilon, \alpha, \delta) = \begin{cases} \dfrac{\varepsilon}{\delta^{1-\alpha}}, & |\varepsilon| \le \delta \\ \text{sign}(\varepsilon)|\varepsilon|^{\alpha}, & |\varepsilon| > \delta \end{cases} \quad (15)$$

The nonlinear state error feedback control law is

$$\begin{aligned} u_0 = &\beta_1 \text{fal}(e_1, \alpha_1, \delta) + \beta_2 \text{fal}(e_2, \alpha_2, \delta) + \\ &\beta_3 \text{fal}(e_3, \alpha_3, \delta) \end{aligned} \quad (16)$$

where fal() is formulated as Eq. (15), $e_1 = v_1 - z_1$, $e_2 = v_2 - z_2$, e_3 is generated by e_1, $\beta_1, \beta_2, \beta_3$, $\alpha_1, \alpha_2, \alpha_3$, δ are all the modified parameters.

Neural network is designed for nonlinear error feedback control law parameter $\beta_1, \beta_2, \beta_3$. Let $x_1 = \text{fal}(e_1, \alpha_1, \delta)$, $x_2 = \text{fal}(e_2, \alpha_2, \delta)$, $x_3 = \text{fal}(e_3, \alpha_3, \delta)$, in which $e(k) = v_0(k) - y(k)$ is monitor signal, through where the neurons generate control signals.

$$u_0(k) = u_0(k-1) + K\sum_{i=1}^{3} \beta_i(k) x_i(k) \quad (17)$$

where K is ratio; $\beta_i(k)$ is corresponding coefficient. Define the performance index as $J_c = 0.5e^2(k)$, then the adjustment quantity of weight coefficient is

$$\begin{aligned} \Delta\beta_i(k) = &-\eta_i \frac{\partial J_c}{\partial \beta_i} = -\eta_i \frac{\partial J_c}{\partial y}\frac{\partial y}{\partial u}\frac{\partial u}{\partial \beta_i} \approx \\ &\eta_i e(k)\frac{\partial y_m}{\partial u} x_i(k) \end{aligned} \quad (18)$$

Therefore, the weight coefficient expression could be adjusted as

$$\beta_1(k) = \beta_1(k-1) + \eta_1 e(k)\frac{\partial y_m}{\partial u} x_1(k) \quad (19)$$

$$\beta_2(k) = \beta_2(k-1) + \eta_2 e(k)\frac{\partial y_m}{\partial u} x_2(k) \quad (20)$$

$$\beta_3(k) = \beta_3(k-1) + \eta_3 e(k)\frac{\partial y_m}{\partial u} x_3(k) \quad (21)$$

where η_1, η_2, η_3 are the learning rates of corresponding weight coefficients, respectively. By setting the learning rates, the system can always be stable and real-time self-tuning of weight coefficients $\beta_1, \beta_2, \beta_3$. The proportional coefficient K can be adjusted in real time according to the needs of the system: too small K will lead to slow response speed of the system and increase the steady-state error of the system; with the increase of K, the response speed increases and the tracking performance is good, but overshoot easily occurs, and too large will cause the system fluctuation.

3 Simulation and Experiment

3.1 Simulation research

MATLAB/Simulink is used to establish the simulation model of ADRC and RBF-ADRC, and the sampling period is set as h=0.01 s. Step signals are used for positioning control and sinusoidal signals for tracking control. The simulation results of the two algorithms are shown in Fig. 7 and Fig. 8 respectively.

The results of the simulation experiment are shown in Tab. 1. In the position control, the step rise time of the ADRC algorithm is 0.4 s, while RBF based ADRC, the step rise time was 0.3 s, the overshoot was 0, and the steady-state error was 0. In tracking control, when the frequency of input sinusoidal signal increases from 0.1 Hz to 0.2 Hz, the maximum deviation of ADRC increases from 3 mm to 7 mm, and the delay time increases from 0.2 s to 0.5 s, while the RBF based ADRC increases the maximum error from 3 mm to 5 mm, and the lag time increases from

0.2 s to 0.3 s. Simulation results show that RBF based ADRC could realize real-time online adjustment of parameters, as well as speeding up response time and improving the precision of control system compared with ADRC.

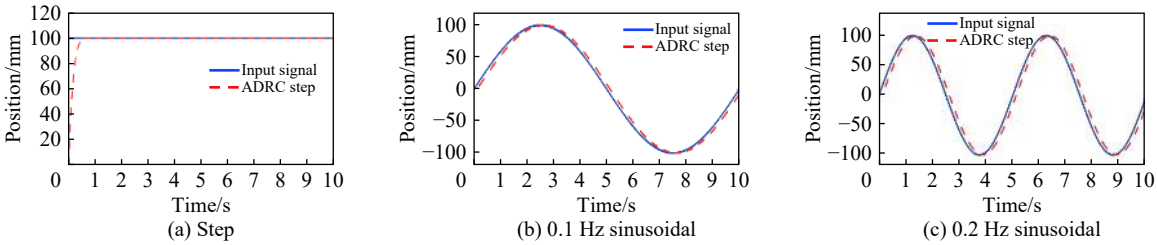

Fig. 7 ADRC experiment results of step/0.1 Hz/0.2 Hz sinusoidal tracking simulation

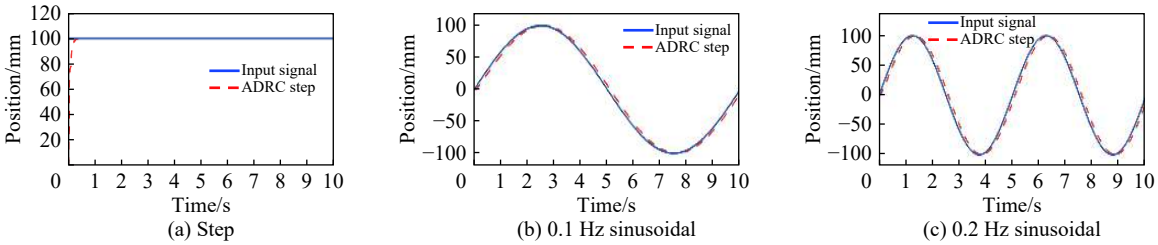

Fig. 8 RBF-ADRC experiment results of step/0.1 Hz/0.2 Hz sinusoidal tracking simulation

Tab. 1 Comparison of simulation experiments ofADRC and RBF-ADRC

Control method	Input signal	Time standard	Indicator
ADRC	Step	Risetime 0.4 s	Overshoot 0, steady-error 0
	0.1 Hz sinusoidal	Lag time 0.2 s	Maximum deviation 3 mm
	0.2 Hz sinusoidal	Lag time 0.5s	Maximum deviation 7 mm
RBF-ADRC	Step	Risetime 0.3 s	Overshoot 0, steady-error 0
	0.1 Hz sinusoidal	Lag time 0.2 s	Maximum deviation 3 mm
	0.2 Hz sinusoidal	Lag time 0.3 s	Maximum deviation 5 mm

3.2 Experimental research

We used the positive cover proportional valve, the flow characteristics are shown in Fig. 3. The actuator of system is ordinary hydraulic cylinder with high friction, so as to reduce the cost of the proportional valve-controlled hydraulic cylinder position servo control system. When the input signal amplitude is 50 mm and the frequency is 0.1 Hz, the tracking performance of RBF-ADRC under the condition of no dead zone compensation and dynamic dead zone compensation are shown in Fig. 9.

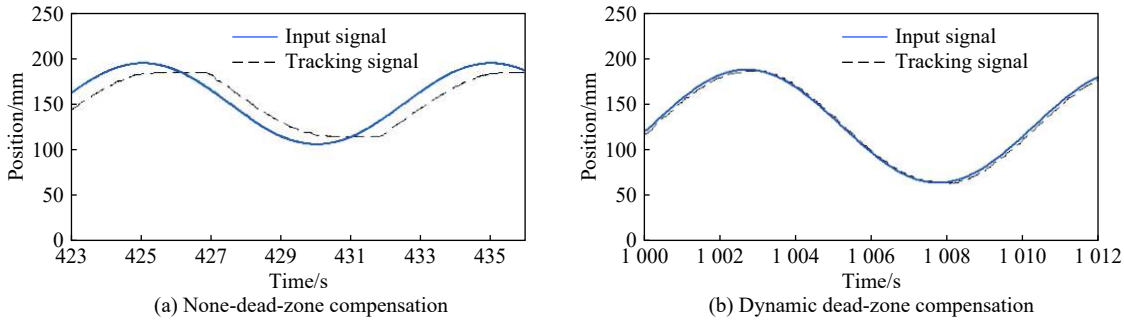

Fig. 9 Tracking performance of RBF-ADRC with none-dead-zone compensation and dynamic dead-zone compensation

According to Fig. 9, under the condition of none-dead-zone compensation, the lag time is 1.5 s with serious flat-top, with a maximum deviation of 20 mm. Because the large dead-zone and great

friction nonlinear characteristics of proportional valve-controlled hydraulic cylinder system, in the process of commutation between extension and contraction, the dead zone and friction impact a lot. When the dead zone dynamic compensation algorithm is added, the flat-top is eliminated, the lag time is 0.2 s, and the maximum deviation is 3 mm, which improves the impact of the system's dead zone characteristics and the control accuracy.

The ADRC and RBF-ADRC control are compared under the condition of dead zone dynamic compensation. The step response amplitude is 150 mm, the sinusoidal tracking amplitude is 50 mm, and the frequency is 0.1 Hz and 0.2 Hz respectively. The experimental results are shown in Fig. 10 and Fig. 11, respectively.

Experimental results of ADRC and RBF-ADRC are shown in Tab. 2.

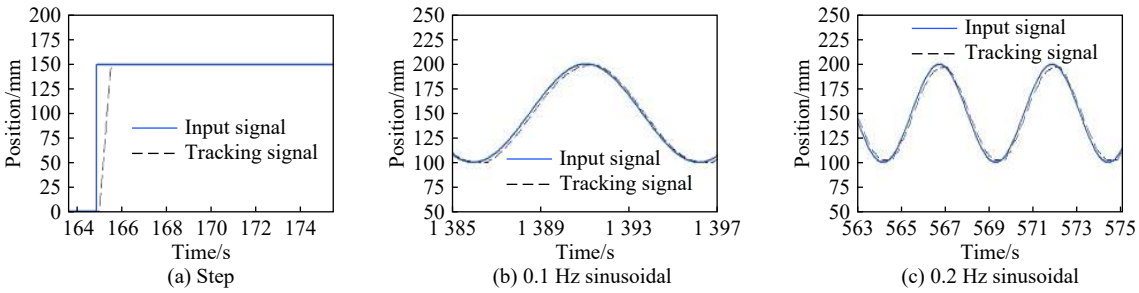

Fig. 10 ADRC response experimental curves with step/0.1 Hz sinusoidal/0.2 Hz sinusoidal

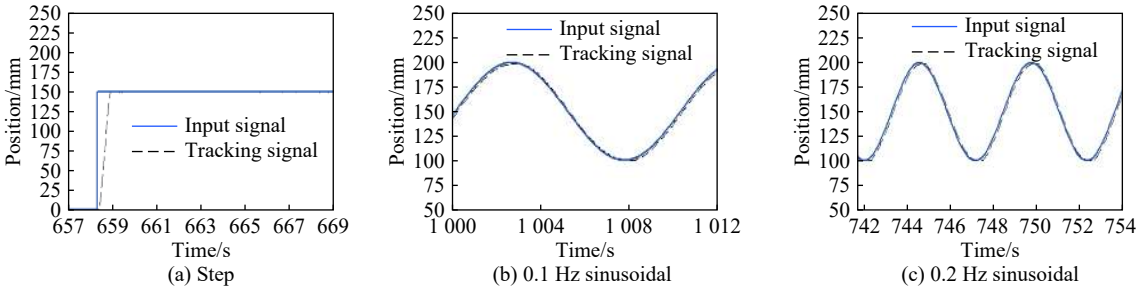

Fig. 11 RBF-ADRC response experimental curves with step/0.1 Hz sinusoidal/0.2 Hz sinusoidal

Tab. 2 Experimental results comparison of ADRC and RBF-ADRC

Control method	Simulation signal	Time standard	Indicator
ADRC	Step	Risetime 0.6 s	Overshoot 0, steady-error 0
	0.1 Hz sinusoidal	Lag time 0.1 s	Maximum deviation 5.0 mm
	0.2 Hz sinusoidal	Lag time 0.3 s	Maximum deviation 6.5 mm
RBF-ADRC	Step	Risetime 0.6 s	Overshoot 0, steady-error 0
	0.1 Hz sinusoidal	Lag time 0.1 s	Maximum deviation 3 mm
	0.2 Hz sinusoidal	Lag time 0.2 s	Maximum deviation 5 mm

The step response results of ADRC and RBF-ADRC are the same, the rise time is 0.6 s, the overshot is 0, and the steady-state deviation is 0. For sinusoidal tracking control at 0.1 Hz, the maximum tracking error of RBF-ADRC is 3 mm, while that of ADRC is 5 mm. The maximum tracking deviation of RBF-ADRC and ADRC is 5.0 mm and 6.5 mm, respectively. Experimental results show that RBF-ADRC could realize real-time adjustment of parameters, improving the precision of control system, and the overall control performance is better than ADRC.

4 Conclusions

① Aiming at the impact of dead zone, friction and other nonlinear characteristics on the control accuracy of the valve controlled hydraulic cylinder system, dead zone dynamic compensation algorithm is proposed to eliminate the flat-top of sinusoidal signal tracking, reducing the lag time and the maximum tracking deviation from 20 mm to 3 mm.

② On the basis of dead zone dynamic compensation, RBF algorithm is introduced to optimize the parameters of ADRC in view of the fact that the ADRC algorithm has many parameters and is difficult to adjust and the accuracy is difficult to guarantee. Simulation experiments show that the optimized ADRC algorithm can automatically adjust parameters, so that the control performance of input sinusoidal signals of 0.1 Hz and 0.2 Hz, the maximum deviation is 3 mm and 5 mm respectively, which improves the control accuracy and adaptability of the system simultaneously.

References:

[1] Wang J, He L, Sun M. Application of active disturbance rejection control to integrated fight-propulsion control[C]//Proceedings of the 22nd Chinese Control and Decision Conference, 2010: 2565-2569.

[2] Xiong H, Yi J, Fan G. Auto-landing of unmanned aerial vehicles based on active disturbance rejection control[C]//Proceedings of the IEEE International Conference on Intelligent Computing and Intelligent Systems, 2009: 772-776.

[3] Sun B, Gao Z. A DSP-based active disturbance rejection control design for a 1-kW H-bridge DC-DC power converter [J]. IEEE Transactions on Industrial Electronics, 2005, 52: 1271-1277.

[4] Dong P, Ye G, Wu J. Auto-disturbance rejection controller in the wind energy conversion system[C]//Proceedings of the Power Electronics and Motion Control Conference, 2004: 878-881.

[5] Li S, Liu Z. Adaptive speed control for permanent-magnet synchronous motor system with variations of load inertia [J]. IEEE Transactions on Industrial Electronics, 2009, 56: 3050-3059.

[6] Long Z, Li Y, Wang X. On maglev train automatic operation control system based on auto-disturbance-rejection control algorithm[C]//Proceedings of the 27th Chinese Control Conference, 2008: 681-685.

[7] Gao Qiang, Hou Yuanlong, Qian Linfang, et al. Application of active disturbances rejection control in electro-hydraulic position servo system of pump-controlled cylinder [J]. Electric Drive & Automatic Control, 2008, 30(3): 15-16.

[8] Guo Dong, Fu Yongling, Lu Ning, et al. Application of ADRC technology in electrohydraulic force servo system [J]. Journal of Beijing University of Aeronautics and Astronautics, 2013, 39(1):115-119. (in Chinese)

[9] Chen Qinghong, Qin Datong. Neural-networked three-parameter gear-shift schedule for automated-manual-transmission car [J]. Control Theory & Application, 2010, 27(11): 1580-1584.

[10] Zhang Haili, Chen Ling. Discussion of the nonlinear compensation technology for electro-hydraulic proportional directional valve [J]. Chinese Hydraulics and Pneumatics, 2008(3): 58-60.

[11] Li Kuangcheng. Adaptive auto disturbance rejection control for servo systems based on the RBF neural network [J]. Intelligent Control Techniques, 2010, 32(2): 23-25.